

A relationship between the waveguide invariant and wavenumber integration

Kevin L. Cockrell^{a)} and Henrik Schmidt

Department of Mechanical Engineering, Massachusetts Institute of Technology, Cambridge, Massachusetts 02139
cockrell@mit.edu, henrik@mit.edu

Abstract: The waveguide invariant is typically defined using of normal modes or ray theory, but it can also be related to the wavenumber-integration method for calculating the acoustic field in a waveguide. In this letter, the Wiener–Khinchin Theorem is used to show that the autocorrelation of the wavenumber-integration kernel, when plotted versus wavenumber difference and frequency, contains striations that can be described by the waveguide invariant.

© 2010 Acoustical Society of America

PACS numbers: 43.30.Bp [JL]

Date Received: March 7, 2010 Date Accepted: May 24, 2010

1. Introduction

A plot of acoustic intensity versus range and frequency in a waveguide with a broadband source will contain striations that are characterized by the waveguide invariant β (Chuprov, 1982). Such striations have been the basis for several methods of acoustic sensing in the ocean including passive source localization (Thode, 2000), array processing (Tao and Krolik, 2008), time-reversal focusing (Kim *et al.*, 2003), and active sonar (Quijano *et al.*, 2008).

Although the waveguide invariant is usually derived and interpreted using normal modes (Brekhovskikh and Lysanov, 2003), ray theory can also be used to interpret the waveguide invariant (Chuprov, 1982; Gerstoft *et al.*, 2001; Brown *et al.*, 2005). The present analysis relates the waveguide invariant to another common method for calculating the acoustic field in a waveguide: wavenumber integration. It will be shown that under certain circumstances, the waveguide invariant can be “seen” in a plot of the autocorrelation of the wavenumber-integration kernel. This result has an intuitive interpretation because the autocorrelation of the wavenumber-integration kernel represents horizontal wavenumber differences, which is what the waveguide invariant is defined in terms of when using a normal mode description of the acoustic field.

The present analysis is for a range independent waveguide with planar geometry so that the wavenumber transform is a Fourier transform (as opposed to a Bessel transform for cylindrical geometry). Because the usual derivation of the waveguide invariant ignores cylindrical spreading, assuming planar geometry is not a limitation.

2. The waveguide invariant and normal modes

Section 6.7.2 of Brekhovskikh and Lysanov, 2003 uses normal modes to derive the waveguide invariant in a waveguide with a point source (cylindrical geometry). Here we present a similar derivation, but we use a planar geometry. For planar geometry, the complex pressure can be written as shown in Eq. 5.26 of Jensen *et al.*, 2000.

^{a)} Author to whom correspondence should be addressed.

$$p(x, z, \omega) \propto \sum_m \psi_m(z_s) \psi_m(z) \frac{e^{ik_{xm}(\omega)|x|}}{k_{xm}(\omega)}, \quad (1)$$

where x is the coordinate pointing directly away from the source and $k_{xm}(\omega)$ is the horizontal wavenumber for mode m at a temporal frequency of ω . For notational convenience define

$$B_m \equiv \psi_m(z_s) \psi_m(z) \frac{1}{k_{xm}(\omega)}. \quad (2)$$

The scalar acoustic intensity is then the pressure times its complex conjugate:

$$I(x, \omega) = p(x, \omega) \cdot \bar{p}(x, \omega) \propto \left(\sum_m B_m e^{ik_{xm}(\omega)x} \right) \cdot \left(\sum_n B_n e^{-ik_{xn}(\omega)x} \right), \quad (3)$$

$$= \left(\sum_q B_q^2 + 2 \sum_{m \neq n} B_m B_n \cos(\Delta k_{mn}(\omega)x) \right), \quad (4)$$

where the overline indicates a complex conjugate and $\Delta k_{mn}(\omega) = k_{xm}(\omega) - k_{xn}(\omega)$. Equation (4) shows that the intensity at a fixed ω is a sum of cosines, each of which has a spatial frequency in the x coordinate that depends on the difference between a pair of modes' horizontal wavenumbers.

In an ideal waveguide, the waveguide invariant states that $\Delta k_{mn}(\omega) \propto 1/\omega$ for modes far from cutoff, which implies that the x -coordinate spatial frequencies in the intensity depend on ω like $1/\omega$ (Grachev, 1993).

3. Relating the waveguide invariant to wavenumber integration

In the previous section it was shown that the x -coordinate spatial frequencies in the acoustic intensity are determined by horizontal wavenumber differences. In this section, we relate the wavenumber integration kernel to the x -coordinate spatial frequencies in the intensity $I(x, \omega)$, which reveals a relationship between the wavenumber integration kernel and the waveguide invariant.

To obtain the complex pressure $p(x, \omega)$ using wavenumber integration, the Helmholtz equation for $p(x, \omega)$ is transformed into the wavenumber domain using the Fourier transform pair [Eqs. 2.85 and 2.86 of Jensen *et al.*, 2000]:

$$p(x) = \int_{-\infty}^{\infty} \Psi(k_x) e^{ik_x x} dk_x, \quad (5)$$

$$\Psi(k_x) = \frac{1}{2\pi} \int_{-\infty}^{\infty} p(x) e^{-ik_x x} dx. \quad (6)$$

The boundary conditions are then written as a function of k_x , and the resulting equations are solved in the k_x wavenumber domain at a single temporal frequency to yield the wavenumber kernel $\Psi(k_x, \omega)$, which represents the magnitude and phase of the spatial frequency components k_x of the complex pressure field at a particular temporal frequency ω . $\Psi(k_x, \omega)$ is then transformed (back) to the x domain using Eq. (5), yielding $p(x, \omega)$. The scalar acoustic intensity can then be computed by multiplying the pressure by its complex conjugate: $I(x, \omega) = p(x, \omega) \cdot \bar{p}(x, \omega)$. Note that the wavenumber kernel $\Psi(k_x, \omega)$ for a cylindrical geometry is identical to that for a planar geometry; only the integral transform used to obtain $p(x, \omega)$ from $\Psi(x, \omega)$ is different.

In order to relate the waveguide invariant to the wavenumber integration kernel $\Psi(k_x, \omega)$, we seek to establish a relationship between $\Psi(k_x, \omega)$ and the x -coordinate spatial frequencies in the intensity $I(x, \omega)$. This relationship is provided by the Wiener–Khinchin Theo-

rem (Weisstein, 2009a, 2009b), which will now be used to show that the magnitude of x -coordinate spatial Fourier transform of $I(x, \omega)$ can be calculated from the autocorrelation of the wavenumber kernel. Note that although the Wiener-Khinchin Theorem is well-known for its use in statistical spectrum estimation, our application is purely deterministic.

The autocorrelation of the wavenumber kernel is:

$$C(\Delta k_x) = \int_{-\infty}^{\infty} \bar{\Psi}(k_x) \Psi(k_x + \Delta k_x) dk_x, \quad (7)$$

where the overline indicates a complex conjugate. Following the standard derivation of the Wiener-Khinchin Theorem, insert Eq. (6) into Eq. (7) and perform a series of algebraic manipulations (Weisstein, 2009a, 2009b):

$$\begin{aligned} C(\Delta k_x) &= \int_{-\infty}^{\infty} \left(\frac{1}{2\pi} \int_{-\infty}^{\infty} \bar{p}(x_1) e^{ik_x x_1} dx_1 \right) \left(\frac{1}{2\pi} \int_{-\infty}^{\infty} p(x_2) e^{-i(k_x + \Delta k_x)x_2} dx_2 \right) dk_x, \quad (8) \\ &= \frac{1}{4\pi^2} \int_{-\infty}^{\infty} \int_{-\infty}^{\infty} \int_{-\infty}^{\infty} \bar{p}(x_1) e^{ik_x x_1} p(x_2) e^{-i(k_x + \Delta k_x)x_2} dk_x dx_1 dx_2 \\ &= \frac{1}{4\pi^2} \int_{-\infty}^{\infty} \int_{-\infty}^{\infty} \int_{-\infty}^{\infty} \bar{p}(x_1) p(x_2) e^{ik_x(x_1 - x_2)} e^{-i\Delta k_x x_2} dk_x dx_1 dx_2 \\ &= \frac{1}{4\pi^2} \int_{-\infty}^{\infty} \int_{-\infty}^{\infty} \bar{p}(x_1) \delta(x_1 - x_2) p(x_2) e^{-i\Delta k_x x_2} dx_1 dx_2 \\ &= \frac{1}{4\pi^2} \int_{-\infty}^{\infty} \bar{p}(x_1) p(x_1) e^{-i\Delta k_x x_1} dx_1 \\ &= \frac{1}{4\pi^2} \int_{-\infty}^{\infty} I(x_1) e^{-i\Delta k_x x_1} dx_1. \quad (9) \end{aligned}$$

Equation (9) shows that the autocorrelation of the wavenumber kernel is proportional to the x -coordinate spatial Fourier transform of the scalar acoustic intensity $I(x)$. If one were to decompose $I(x)$ into all of its spatial frequencies components, the relative magnitude of those spatial frequencies could be determined by the autocorrelation of the wavenumber kernel.

This result can be related to the normal modes description of the acoustic intensity given in Eq. (4). The wavenumber kernel $\Psi(k_x)$ has peaks at values of k_x corresponding to the modal horizontal wavenumbers. Thus the autocorrelation of $\Psi(k_x)$ will be large at Δk_x values corresponding to the *differences* in the modal horizontal wavenumbers—precisely the x -coordinate spatial frequencies of $I(x, \omega)$ shown in Eq. (4).

The peaks (local maxima) of the autocorrelation of the wavenumber kernel correspond to the modal horizontal wavenumber differences ($\Delta k_{mn}(\omega)$), so the peaks' dependence on frequency will be the same as $\Delta k_{mn}(\omega)$'s dependence on frequency. Because the waveguide invariant describes $\Delta k_{mn}(\omega)$'s dependence on frequency, the waveguide invariant also describes how the peaks of the autocorrelation of the wavenumber kernel depend on frequency. The next section analyzes this further.

4. An ideal example

The waveguide invariant is well understood for an ideal waveguide because the horizontal wavenumbers can be calculated analytically. For mode pairs in an ideal waveguide where both modes are far from cutoff, $\Delta k_{mn}(\omega)$ is approximately proportional to $1/\omega$, which corresponds to

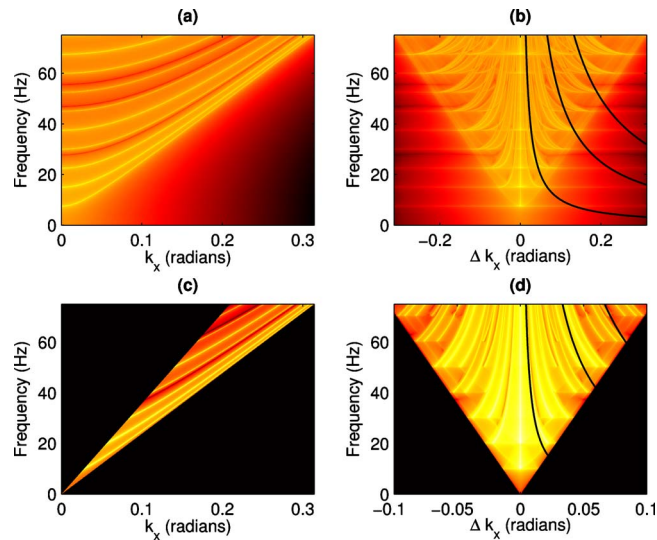


Fig. 1. (Color online) All subfigures are for a 100 m deep ideal waveguide with $z_s=16$ m and $z=73$ m, and are in units of dB re: an arbitrary reference. (a) $|\Psi(k_x, \omega)|$, the wavenumber kernel as a function of horizontal wavenumber and frequency. (b) $|C(\Delta k_x, \omega)|$, the autocorrelation of wavenumber kernel shown in subfigure (a) as a function of wavenumber difference Δk_x and frequency ω . The black lines are example striation paths corresponding $\beta=1$ (lines with $\Delta k_x \propto 1/\omega$). (c) Same as subfigure (a), but only including k_x values far from cutoff ($\frac{2}{3}k < k_x < k$). (d) $|C(\Delta k_x, \omega)|$, the autocorrelation of the wavenumber kernel shown in subfigure (c). The black lines are example striation paths corresponding $\beta=1$ (lines with $\Delta k_x \propto 1/\omega$), and match the actual striation paths more closely than those in subfigure (b) because subfigure (d) only includes k_x values far from cutoff.

$\beta \approx 1$ [Eq. 6.7.34 of Brekhovskikh and Lysanov, 2003 and Grachev, 1993]. So one would expect the Δk_x location of the peaks in $C(\Delta k_x, \omega)$ for an ideal waveguide to depend on ω like $1/\omega$. We now show that this is indeed the case.

The wavenumber kernel for an ideal waveguide is [Eq. 2.143 of Jensen *et al.*, 2000]

$$\Psi(k_x, \omega) \propto \begin{cases} \frac{\sin k_z z \sin k_z (D - z_s)}{k_z \sin k_z D}, & z < z_s \\ \frac{\sin k_z z_s \sin k_z (D - z)}{k_z \sin k_z D}, & z > z_s, \end{cases} \quad (10)$$

where $k_z = \sqrt{(\omega/c)^2 - k_x^2}$ and D is the depth of the waveguide. $\Psi(k_x, \omega)$ has poles when $k_z D = m\pi$ for positive integers m , or equivalently at k_x values corresponding to the modal horizontal wavenumbers. Those poles will then depend on frequency in the same manner as the modal horizontal wavenumbers will, and so the Δk_x location of the peaks of $C(\Delta k_x, \omega)$ will depend on ω in the manner predicted by the waveguide invariant ($\propto 1/\omega$).

To visualize this dependence, a plot of $\Psi(k_x, \omega)$ is shown in Fig. 1(a) along with its autocorrelation in Fig. 1(b). The black lines in Fig. 1(b) correspond to a few potential striation paths predicted by the waveguide invariant with $\beta=1$ (lines with $\Delta k_x \propto 1/\omega$). It can be seen that there are striations in Fig. 1(b) that do not match up well with the black lines. This discrepancy appears to contradict the analysis in the previous section. But if we remember that β is only approximately equal to 1 for mode pairs where both modes are far from cutoff, or equivalently when k_x is close to k , then the discrepancy makes sense because the wavenumber kernel contains horizontal wavenumber components that are close to cutoff and thus are not well described by $\beta=1$. To address this issue, Fig. 1(c) shows the wavenumber kernel using only k_x values close

to k (specifically, $\frac{2}{3}k < k_x < k$) and Fig. 6(d) shows the resulting autocorrelation along with black lines corresponding to $\beta=1$. The striations in Fig. 1(d) match very well with the black lines because only horizontal wavenumbers that are far from cutoff are included.

5. Relevance

Many applications of the waveguide invariant require an assumption about the value of β . It is often correct to assume that $\beta \approx 1$ in shallow-water waveguides, but this assumption is not always valid (Chuprov, 1982). Consequently, numerical modeling is sometimes used to determine the approximate value of β in a given environment (Rouseff and Spindel, 2002). Although this can be done by simulating the acoustic field itself, more insight can often be gained by calculating more fundamental quantities such as the modal horizontal wavenumbers or the ray parameters (horizontal slowness, cycle distance, etc.—see Eqs. 11–15 of Gerstoft *et al.*, 2001), which can be related to the value of the waveguide invariant.

However, normal modes and ray theory are not conducive to describing the acoustic field in some environments, such as those involving attenuating elastic media (especially if one is interested in the acoustic field inside of the elastic media). In those cases, understanding how the wavenumber-integration kernel relates to the waveguide invariant may allow one to gain insights that would be difficult to obtain otherwise.

For example, the concepts described in this letter may be useful for studying the effect that surface ice has on the value of β . The striations in a plot like Fig. 1(d), but generated for an ice-covered waveguide rather than an ideal one, could reveal whether it's reasonable to assume $\beta=1$ in such an environment. More specifically, one could use a plot like Fig. 1(d) to determine if hydrophones sitting on surface ice (or embedded in the seafloor) would record the same range-frequency waveguide invariant striations that a hydrophone in the water column would record.

6. Summary

The waveguide invariant implies a specific dependence of the acoustic intensity's x-coordinate spatial frequencies on the temporal frequency ω . When the geometry of the problem is planar, the wavenumber integration transform is a Fourier Transform, and so the Wiener–Khinchin Theorem can be used to relate the autocorrelation of the wavenumber kernel to the x-coordinate spatial frequencies in the acoustic intensity. A 2-d plot of the autocorrelation of the wavenumber kernels versus “wavenumber lag” Δk_x and temporal frequency ω exhibits striation patterns that can be explained by the waveguide invariant.

The relationship between the waveguide invariant and wavenumber integration is not as direct as the waveguide invariant's relationship to normal using modes or ray theory. However, the relationship described in the present analysis may be useful in certain situations because wavenumber integration can be used in waveguides that are difficult to model using normal modes or ray theory.

Acknowledgments

Work sponsored by the Office of Naval Research under Grant No. N00014-08-1-0013. The authors thank the reviewers for their comments.

References and links

- Brekhovskikh, L. M., and Lysanov, Yu. P. (2003). *Fundamentals of Ocean Acoustics*, 3rd ed. (AIP, New York / Springer, New York).
- Brown, M. G., Beron-Vera, F. J., Rypina, I., and Udovydchenkov, I. A. (2005). “Rays, modes, wavefield structure, and wavefield stability,” *J. Acoust. Soc. Am.* **117**, 1607–1610.
- Chuprov, S. D. (1982). “Interference structure of a sound field in a layered ocean,” in *Ocean Acoustics. Current State*, edited by L. M. Brekhovskikh and I. B. Andreeva (Nauka, Moscow).
- Gerstoft, P., D’Spain, G. L., Kuperman, W. A., and Hodgkiss, W. S. (2001). “Calculating the waveguide invariant (beta) by ray-theoretic approaches,” MPL Technical Memo No. TM-468, Marine Physical Laboratory, University of California, San Diego.
- Grachev, G. A. (1993). “Theory of acoustic field invariants in layered waveguides,” *Acoust. Phys.* **39**, 33–35.

- Jensen, F. B., Kuperman, W. A., and Porter, M. B., and Schmidt, H. (2000). *Computational Ocean Acoustics* (AIP, New York /Springer, New York).
- Kim, S., Kuperman, W. A., Hodgkiss, W. S., Song, H. C., Edelmann, G. F., and Akal, T. (2003). "Robust time reversal focusing in the ocean," *J. Acoust. Soc. Am.* **114**, 145–157.
- Quijano, J. E., Zurk, L. M., and Rouseff, D. (2008). "Demonstration of the invariance principle for active sonar," *J. Acoust. Soc. Am.* **123**, 1329–1337.
- Rouseff, D., and Spindel, R. C. (2002) "Modeling the waveguide invariant as a distribution," *AIP Conf. Proc.* **621**, 137150.
- Tao, H., and Krolik, J. L. (2008). "Waveguide invariant focusing for broadband beamforming in an oceanic waveguide," *J. Acoust. Soc. Am.* **123**, 1338–1346.
- Thode, A. M., Kuperman, W. A., D'Spain, G. L., and Hodgkiss, W. S. (2000). "Localization using Bartlett matched-field processor sidelobes," *J. Acoust. Soc. Am.* **107**, 278–286.
- Weisstein, E. W. (2009a). "Wiener-Khinchin theorem," <http://mathworld.wolfram.com/Wiener-KhinchinTheorem.html> (Last viewed 11/10/09).
- Weisstein, E. W. (2009b). "Cross-correlation theorem," <http://mathworld.wolfram.com/Cross-CorrelationTheorem.html> (Last viewed 11/10/09).